Magnetic field-induced Freedericksz transition in a chiral liquid crystal

Amine Missaoui[1], Adam L. Susser[1], Hillel Aharoni[2], and Charles Rosenblatt[1]

1. **Department of Physics, Case Western Reserve University, Cleveland, Ohio 44106 USA**
2. **Department of Complex Systems, Weizmann Institute of Science, Rehovot, Israel**

Abstract

A wedge cell made of homeotropically treated glass plates is filled with a chirally-doped nematic liquid crystal (LC). When a sufficiently large magnetic field is applied in the cell plane, a bend-like distortion occurs above a Freedericksz threshold field H_{th}. H_{th} is reduced from the achiral case because of a field-induced bend distortion that facilitates a chiral twist distortion. Measurements of H_{th} vs. sample thickness are reported and compare favorably with a theoretical model presented herein. A further theoretical comparison is made between H_{th} and the electric-field-induced transition in a geometry exhibiting a 2π azimuthal degeneracy. The results may have technological implications in, for example, in-plane switching devices.

Introduction

The unique photonic and electro-optical properties of chiral liquid crystals have attracted much attention and have made them widely used materials in many fields, including LC displays, voltage modulated transparency eyeglasses, temperature visualization, and lasing [1-12]. The chiral “cholesteric phase” is distinguished from the nematic phase by a helical director field twisted along a well-defined axis perpendicular to the local director field. The spatial period over

which the director twists by 2π is called the chiral pitch *p*; the nematic phase corresponds to $p \rightarrow \infty$.

When an electric field is applied in an appropriate direction relative to a uniformly aligned nematic liquid crystal filled between two substrates, there is competition between the electric field energy and the elastic energy of the LC. The elastic energy stabilizes the uniform alignment of the LC below a threshold field E*th* that depends on the physical properties of the LC and the cell thickness *L*; above the threshold field, director field fluctuations facilitate what is known as a "Freedericksz transition" [13]. This phenomenon was the basis for some of the earliest LC displays. Additionally, it has been shown that a magnetic field may also induce a Freedericksz transition [13-15] due to the LC's diamagnetic susceptibility anisotropy, which is almost always positive.

For an appropriate geometry, the use of a chiral LC can reduce the Freedericksz threshold electric field [16-19]. Consider a sufficiently small confinement ratio $c \equiv L / p$ so that the director of the cholesteric phase is untwisted to a uniform vertical (also known as homeotropic) alignment along the *z*-axis normal to the cell plane. This phenomenon is an example of "surface stabilization". But a chiral LC prefers to undergo a twist distortion, which requires a director component in the *xy*-plane. This condition can be met only if the uniform vertical alignment is perturbed by a bend distortion, which can be achieved if the LC has a negative dielectric anisotropy $\Delta\varepsilon < 0$ and an electric field is applied along the *z*-axis so that it undergoes a Freedericksz transition. Thus, the propensity of the chiral LC director to twist encourages the appearance of a bend distortion and thus reduces the Freedericksz threshold voltage, which in

principle can even reach zero. This threshold reduction was studied by several groups [16-19], and the behavior of the director field above the threshold voltage was also examined by [17-19].

The above surface-stabilized homeotropic geometry, a negative dielectric anisotropy chiral LC, and an electric field normal to the cell plane is a high symmetry arrangement, as the field-induced tilt of the director above the Freedericksz threshold is 2π azimuthally degenerate; this has only limited practical use and is clearly different from "in-plane switching" (IPS) [20-22] technology. We now ask the question: How might this behavior be modified if the 2π-degeneracy is broken with an in-plane field and a positive anisotropy LC? That is, the applied field not only induces a bend distortion, but the resulting twisted director is biased by the field to orient along a particular direction in the cell plane. This can be achieved experimentally with a $\Delta\varepsilon > 0$ chiral LC and an electric field applied in the cell plane, perpendicular to the surface-stabilized director orientation. However, an in-plane electric field suffers from spatial inhomogeneities, being smallest midway between the electrodes and going to infinity at the electrodes [23]. LCs also respond readily to magnetic fields. Thus, a spatially uniform in-plane *magnetic* field can be applied to a positive diamagnetic susceptibility anisotropy ($\Delta\chi$>0) chiral LC to achieve the desired broken symmetry IPS experimental configuration. Results from magnetic measurements and theory may provide important information on how one can manipulate E_{th} in chiral electric field IPS devices.

In this paper we report the magnetic response of a chiral nematic mixture having $\Delta\chi > 0$, initially surface-stabilized in the homeotropic configuration. By applying an in-plane magnetic field perpendicular to the director, we measure a Freedericksz threshold field H_{th} at which the sample begins to undergo a combination of bend and twist distortions. This H_{th} is lower than for

the achiral nematic. (Note that, for now, we write H_{th} as the generic threshold field for both experimental H_{Exp} and theoretical H_{Theor} threshold field.) We present a theoretical model for this symmetry-broken configuration, finding good agreement with experiment. Additionally, the results are compared to the electric field 2π-degenerate experiments.

Experimental

Experimental details will now be presented. First, the LC cells and their assembly will be described, followed by the experimental apparatus and results. Microscope glass slides of size 1 x 1 cm were cleaned with detergent and water, acetone, and then ethanol. A thin alignment layer of the polyimide SE1211 (Nissan Chemical Industries) was deposited by spin-coating at 3000 rpm for 30 s to promote homeotropic alignment, and then soft baked at 80 °C for 30 min and hard baked at 180 °C for 1 h. A pair of wedge cells were prepared, each consisting of two such slides separated on one end by Mylar spacer of nominal thickness 25 μm and cemented together with epoxy. The actual thickness *L* of the empty cells was determined as a function of position by interferometry [24] and the uniformity by observation of Newton's rings.

Two cells were filled in the isotropic phase, one with pure liquid crystal 4-cyano-4'-pentylbiphenyl (5CB; EM Industries), and the other with a mixture of (0.73 ± 0.03) wt-% chiral dopant CB15 (EM Industries) in 5CB. Both were allowed to cool to room temperature where the nematic phase was observed. The natural pitch of the doped LC was determined by the condition $c \approx 1$, where the LC was no longer surface stabilized [14,17-19], and where we found p = (17 ± 0.5) μm. (This will be discussed in more detail later). Each sample was placed in an electromagnet with transverse optical access and where the magnetic field *H* was oriented parallel to the cell (Fig. 1, inset). Light from a 5 *mW* He-Ne laser passed consecutively through a polarizer, a focusing

lens, the sample, an analyzer, a light chopper used to remove effects of extraneous light, a Babinet–Soleil compensator, and into a detector. The detector output was input to a lock-in amplifier referenced to the chopper frequency. To improve the sensitivity of the optical retardation measurements, the compensator was adjusted so that the optical retardation was approximately $\pi/4$, and thus the optical intensity varied approximately linearly with sample retardation. We then measured the magnetic threshold field for the Freedericksz transition of the two wedge samples on slowly ramping up the field, and the results are shown in see Fig. 1. (The lines show the theoretical values, as will be explained later.)

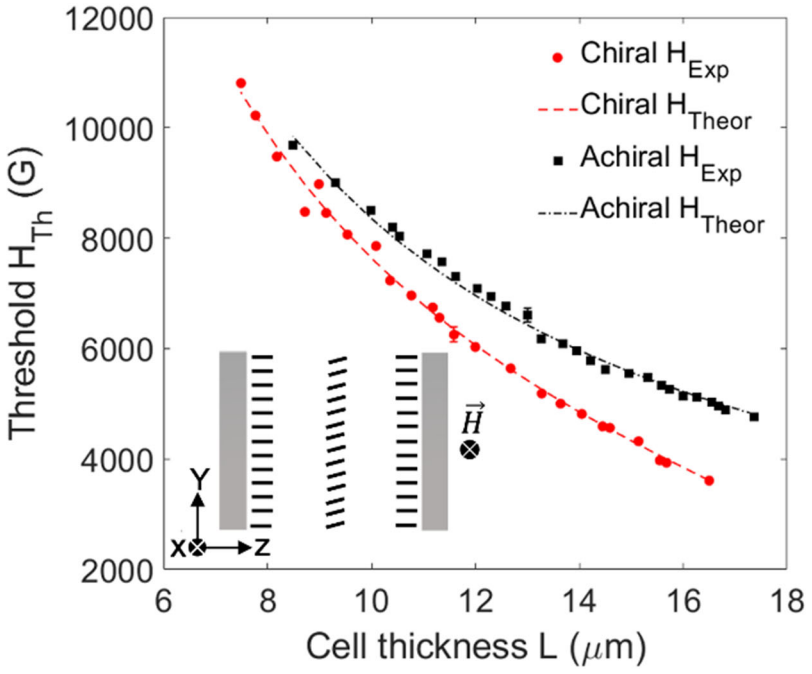

Figure 1: Experimental and theoretical threshold field as a function of the sample thickness L. The chiral and achiral data are shown as red circles and black squares, respectively. Typical error bars are shown. The inset shows a schematic representation of the sample cross section above the Freedericksz threshold field.

Theory

A theoretical model explaining these results will now be presented. Consider a chiral nematic liquid crystal in a cell of constant thickness *L* with strong homeotropic anchoring at the two surfaces $z = \pm L/2$. The chiral nematic has spontaneous twist q_0, elastic twist and bend constants K_{22} and K_{33}, respectively, and positive magnetic susceptibility anisotropy $\Delta\chi$. Subject to a constant magnetic field $\vec{H} = H\hat{x}$, and omitting splay distortions that are expected to vanish in this configuration near the Freedericksz transition, the free energy density is

$$f = \frac{K_{22}}{2}\left(\hat{n}\cdot\vec{\nabla}\times\hat{n} + q_0\right)^2 + \frac{K_{33}}{2}\left|\hat{n}\times\vec{\nabla}\times\hat{n}\right|^2 - \frac{\Delta\chi}{2}(\vec{H}\cdot\hat{n})^2 \quad , \qquad (1)$$

where q_0 is the inverse pitch, viz., $q_0 = 2\pi/p$. We now assume a director field that is independent of the lateral coordinates x, y, and take a single Fourier component, with wavenumber π/L in $\theta(z)$ (as a result of the homeotropic anchoring) and an arbitrary wavenumber *q* in $\phi(z)$. Choosing the phase to respect the π-rotation-about-$\hat{x}$ symmetry owing to the magnetic field, and assuming a small perturbation away from $\hat{n} = \hat{z}$, we obtain

$$\hat{n} = \left(\alpha\cos\left(\pi z/L\right)\cos(qz)\,,\,\alpha\cos\left(\pi z/L\right)\sin(qz)\,,\,1\right) + O(\alpha^2). \qquad (2),$$

where α is the perturbation parameter. Substituting Eq. 2 into Eq. 1 and integrating, we obtain the free energy per unit area $F = \int_{-L/2}^{-L/2} f\,dz$. To write the result in a compact way we first define the following dimensionless parameters:

$$\tilde{F} \equiv \frac{4K_{22}L}{K_{33}^2}F, \qquad \tilde{H} = \frac{L}{\pi}\sqrt{\frac{\Delta\chi}{2K_{33}}}H, \qquad \tilde{\alpha} = \sqrt{\frac{2K_{22}}{K_{33}}}\pi\alpha, \qquad \tilde{q} = \frac{L}{\pi}q, \qquad \tilde{q}_0 = \frac{L}{\pi}\frac{2K_{22}}{K_{33}}q_0.$$

Whence,

$$\tilde{F} = \frac{\pi^2\tilde{q}_0^2}{2} + \left(1 + \tilde{q}^2 - \tilde{q}\tilde{q}_0 - \left[1 + \frac{sinc(\pi\tilde{q})}{1-\tilde{q}^2}\right]\tilde{H}^2\right)\frac{\tilde{\alpha}^2}{2} + O(\tilde{\alpha}^4). \qquad (3)$$

The stability of each mode corresponds to the sign of the $\tilde{\alpha}^2$-coefficient in Eq. 3 (negative is unstable and positive is stable). Thus, we obtain the threshold magnetic field for each mode $\tilde{q}$:

$$\tilde{H}_{Theor}^2(\tilde{q}) = \frac{1+\tilde{q}^2-\tilde{q}\tilde{q}_0}{1+\frac{sinc(\pi\tilde{q})}{1-\tilde{q}^2}} \qquad (4)$$

In Fig. 2 we show the calculated threshold field $\tilde{H}_{Theor}$ vs. all possible modes $\tilde{q}$, calculated from Eq. 4, over a range of chiral concentrations $\tilde{q}_0$. The most unstable mode for each is marked with a dot and corresponds to the theoretical threshold field for the Freedericksz transition. The director field of the homeotropically-aligned LC remains uniform for all H less than this most unstable value of $\tilde{H}_{Theor}$, but undergoes a Freedericksz transition at $H = \tilde{H}_{Theor}$.

In principle, Eq. 4 admits a solution for which $\tilde{H}_{th} \to 0$ for $\tilde{q}_0 = 2$ and the resulting mode $\tilde{q} = 1$. Also note that in the limit $p \to \infty$ and/or $L \to 0$, Eq. 4 reduces to the traditional Freedericksz result $H_{Theor}^2 = \frac{\pi^2}{L^2}\left(K_{33}/\Delta\chi\right)$ [26]. As discussed above, an analogous vanishing

electric field threshold was examined previously [16, 17, 19] in a $\Delta\varepsilon < 0$ LC with the field applied along the z-axis. In that case there was 2π-degenerate symmetry in the xy-plane, unlike our current magnetic field configuration in which this symmetry is broken. (An inverse experiment using a positive dielectric anisotropy to *unwind* a pitch in a large confinement parameter *c=L/p* also has been reported [14]).

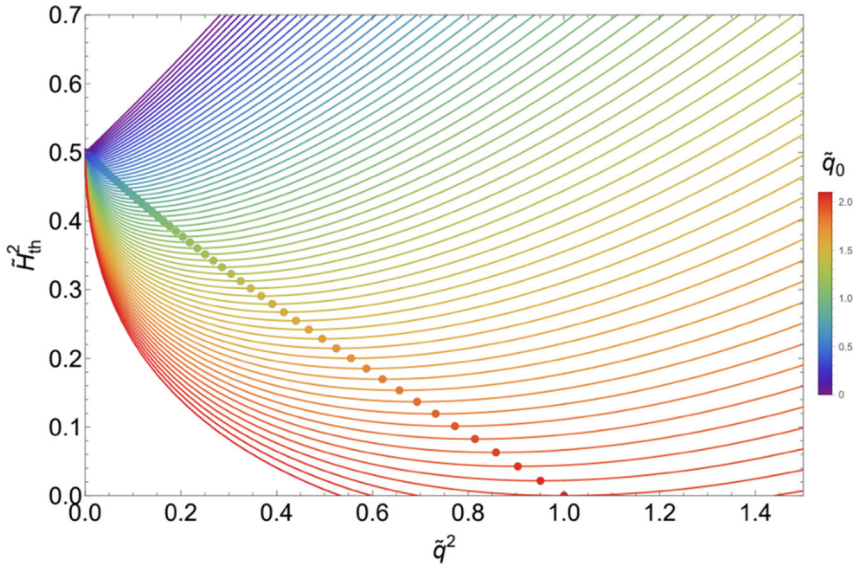

Figure 2: Threshold field of every Fourier mode $\tilde{q}$ for different values of the chiral dopant-induced wavenumber $\tilde{q}_0$. The most unstable mode is marked with a dot and corresponds to the threshold field for the Freedericksz transition.

Discussion

With this theoretical background, the results can now be better understood. When a given sample was subjected to a field $H < H_{Exp}$, the photodetector intensity was effectively zero (within noise), but increased sharply above H_{Exp}, which is a classic Freedericksz intensity result. Figure 1 shows the experimental threshold H_{Exp} and the theoretical threshold H_{Theor} values (from

Eq. 4 and Fig. 2) as a function of the sample thickness *L*. Here we used the parameters *p* = 17 μm, K_{22} = 0.29 x 10^6 dyne, K_{33} = 0.75 x 10^6 dyne and $\Delta\chi$ = 1.06 x 10^{-7} c.g.s. units [25]. Figure 1 shows good agreement between the experimental and theoretical results, with inconsequential effects due to finite anchoring conditions and cell thickness [24]. The black dashed line and the squares represent, respectively, the theoretical and experimental threshold values for the achiral sample. On the other hand, the chiral data are represented by the red dashed line for the theoretical and by the red points for the experimental results.

The above estimate of the pitch *p* ≈ (17 ± 0.5) μm, obtained from the surface stabilization condition *c* = *L*/*p* = 1 [14, 17-19] is different from that obtained using the helical twisting power (HTP) literature values (stated without error bars [27]). From a Cano-wedge experiment [28], we would have obtained a longer pitch *p* ~ 18.7 μm with error bars of at least ±6% due to possible (but unstated) uncertainties in the literature HTP value, in addition to errors due to uncertainties of about ±4% in our chiral dopant concentration. Our own attempt at the Cano-wedge technique with our prepared sample resulted in even larger error bars. Thus, we have chosen to use our more reliable determination of *p* by exploiting the *c* ≈ 1 surface stabilization criterion.

It is of interest to compare lower symmetry theoretical magnetic field result with the higher symmetry theoretical electric field result of Crandall, et al [16]. For the case of the electric field, where 2π symmetry was present, it was shown that the critical thickness $L_c = pK_{33}/2K_{22}$ at which $E_{th} \to 0$ for a chiral LC depends linearly on the pitch *p* [16]. For $L < L_c$, Ref. 16 shows

$$E_{theor}^2 = \frac{\pi^2}{-L^2\Delta\chi}\left(K_{33} - \frac{K_{22}^2 L^2 q_0^2}{K_{33}\pi^2}\right). \qquad (5)$$

The normalized value of $L^2E_{Theor}^2$ vs. L^2 is plotted as the solid blue line in Fig. 3, where the normalization factor is its extrapolated value as $L \rightarrow 0$.

To compare Eq. 5 with our magnetic field theory, we plot in Fig.3 the normalized electric field results V_{th}^2 (i.e., $(LE_{th})^2$ vs. L^2, (left y-axis)) [13], where the normalization factor corresponds to the value as $L \rightarrow 0$. Thus, the *normalized* value of $L^2E_{th}^2$ equals unity at $L = 0$. We also plot the experimental $L^2H^2_{exp}$ and the theoretically calculated $L^2H^2_{Theor}$ normalized values as a function of the square of the cell thickness L^2 (right y-axis), again normalized to the value above when $L \rightarrow 0$, where $H_{Exp} = H_{Theor}$. (Because of these normalizations, the magnetic ($\Delta\chi$) and dielectric ($\Delta\varepsilon$) anisotropies do not appear explicitly and the results from the two types of fields therefore can be compared.) On the other hand, the chiral data are represented by the red dashed line for the theoretical and by the red points for the experimental results.

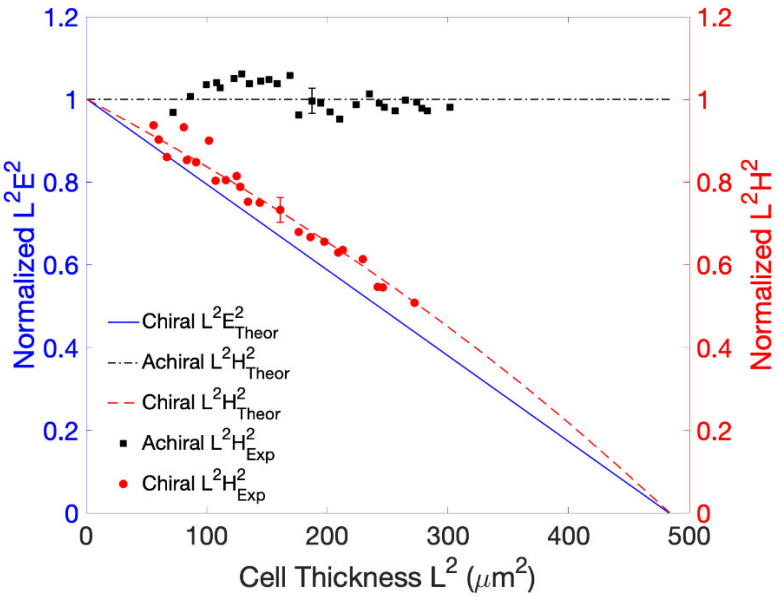

Figure 3: The chiral normalized experimental $L^2H^2_{Exp}$ and normalized theoretical $L^2H^2_{Theor}$ magnetic field results (red, right y-axis), as well as the normalized theoretical electric field $L^2E^2_{Theor}$ (blue, left y-axis), as

a function of L^2 and using a pitch p = 17 μm. The achiral normalized magnetic data and theory are shown in black. Typical error bars are shown.

As expected, the electric field quantity is linear in L^2, as per Eq. 5, whereas the magnetic thresholds are not. The normalized quantities are both equal to unity at $L^2 = 0$ by design, and the normalized $L^2H^2_{Theor}$ and $L^2E^2_{Theor}$ *both* vanish at the same extrapolated critical thickness L_c = 22 μm. (For this LC it is not possible to reach the limit $L = L_c$, as surface director stabilization breaks down well below L_c; however, a LC with a larger K_{22}/K_{33} ratio could make this viable. See, e.g., Eq. 5.) The theoretical L_c result can be understood by noting that, by definition, both E_{Theor} and H_{Theor} vanish at L_c, and therefore the geometry for both cases is 2π degenerate. However, between the two limits of $L^2 = 0$ and $L^2 = L_c^2$ the dependence of $L^2H^2_{Theor}$ on the sample thickness differs from that of $L^2E^2_{Theor}$, suggesting that the additional broken symmetry configuration present in our samples plays an important role for the chiral LC. From Fig. 3 we see that our experimental magnetic field data are consistent with the curvature of the chiral magnetic Freedericksz transition presented above. We note, however, that if a longer pitch estimate (e.g., 18.7 μm) had been used in our magnetic field model calculations, L_c would have been approximately 23.5 μm, and the agreement between chiral experimental magnetic field results and theoretical predictions would have been weaker.

Conclusions

In summary, we studied the Freedericksz transition in a chirally-doped nematic LC in a surface-stabilized homeotropic geometry by applying a spatially uniform, in-plane magnetic field

(i.e., normal to the director). This geometry results in a breaking of the 2π-degeneracy, as a sufficiently large magnetic field induces a bend distortion such that the resulting twisted director is biased to orient along the field direction in the cell plane. Our results show that both the experimental and theoretical Freedericksz threshold fields H_{Exp} and H_{Theor} decrease as the LC pitch p decreases, *i.e.*, at higher chiral dopant concentrations. Our theoretical model takes into account the broken symmetry configuration, and demonstrates good agreement with our experimental results. We also showed that the magnetic response of a chiral nematic mixture with a broken symmetry differs qualitatively from that of the 2π-degenerate electric field response, although relatively weakly. Although this geometry for a spatially-uniform magnetic field Freedericksz transition is not likely to have any direct device applications, the results suggest that an electric field arising from in-plane electrodes (which is inherently spatially nonuniform) may be used in, *e.g.*, in-plane switching (IPS) display devices to good effect: The threshold field E_{th} can be reduced with a chiral dopant and the optics of the twisted director field may be exploitable.

Acknowledgments

CR thanks the Weizmann Institute of Science, Rehovot, Israel for a Weston Visiting Professorship and Ian Stevenson for useful discussions. This work was supported by the National Science Foundation under grant DMR1901797, by the National Aeronautics and Space Administration under grant NNX17AC76G, and by the United States-Israel Binational Science Foundation (BSF) under grant 2018380.

References

[1] L. M. Blinov, and V. G. Chigrinov, Electrooptic Effects in Liquid Crystal, Materials Springer, 309 (1994).

[2] T. J. Scheffer, and J. Nehring, Appl. Phys. Lett. 45, 1021 (1984).

[3] S. Obayya, M. F. O. Hameed, and N. F. F. Areed, Computational Liquid Crystal Photonics: Fundamentals, Modelling and Applications, Wiley & Sons., (2016).

[4] D. Yang, and S. Wu, Fundamentals of Liquid Crystal Devices, Wiley & Sons, (2006).

[5] R. Kumar, and K. K. Raina, Liq. Cryst. 41, 228 (2014).

[6] J. Geng, C. Dong, L. Zhang, Z. Ma, L. Shi, H. Cao, and H. Yang, Appl. Phys. Lett. 89, 081130 (2006).

[7] B. Liu, Z. Zheng, X. Chen, and D. Shen, Opt. Mat. Express. 4, 519 (2013).

[8] M. Kleman, and O.D. Lavrentovich, Soft Matter Physics: An Introduction, Springer, (2003).

[9] O. D. Lavrentovich, and M. Kleman, Chirality in Liquid Crystals, Springer, (2001).

[10] V. I. Kopp, B. Fan, H. K. M. Vithana, and A. Z. Genack, Opt. Lett. 23, 1707 (1998).

[11] J. Schmidtke, and W. Stille, The European Phys. J. B. 31, 179 (2003).

[12] A. Y.-G. Fuh, T.-H. Lin, J.-H. Liu, and F.-C. Wu, Opt. Express. 12, 1857 (2004).

[13] V. Fréedericksz, and A. Repiewa, Zeitschrift für Physik 42, 532 (1927).

[14] P. Oswald, J. Baudry, and S. Pirkl, Phys. Reports, 337, 67-96 (2000).

[15] P. Pincus, J. of App. Phys. 41, 974 (1970).

[16] K. A. Crandall, M. R. Fisch, R. G. Petschek, and C. Rosenblatt, Appl. Phys. Lett. 64, 1741 (1994).

[17] P. Ribière, S. Pirkl, and P. Oswald, Phys. Rev. E. 44, 8198 (1991).

[18] P. Ribiere, and P. Oswald, J. Phys. 51, 1703 (1990).

[19] I. I. Smalyukh, B. I. Senyuk, P. Palffy-Muhoray, O. D. Lavrentovich, H. Huang, E. C. Gartland, Jr., V. H. Bodnar, T. Kosa, and B. Taheri, Phys. Rev. E. 72, 061707 (2005).

[20] R. A. Soref, J. of App. Phys., 45, 5466 (1974).

[21] O. Masahito, and K. Katsumi, Appl. Phys. Lett., 69, 623 (1996).

[22] S. H. Lee, S. L. Lee, and H. Y. Kim, Appl. Phys. Lett., 73, 2881 (1998).

[23] C. Rosenblatt, R.B. Meyer, R. Pindak, and N. A. Clark, Phys. Rev. A. 21, 140 (1980).

[24] C. Rosenblatt, J. Phys. 45, 1087 (1984).

[25] N. V. Madhusudana, and R. Pratibha, Mol. Cryst. Liq. Cryst. 89, 249-257 (1982).

[26] P.G. de Gennes, and J. Prost, The Physics of Liquid Crystals, Clarendon Press, (1993).

[27] M. C. M. Varney, Q. Zhang, B. Senyuk, and I. I. Smalyukh, Phys. Rev. E. 94, 042709 (2016).

[28] D. Podolskyy, O. Banji, and P. Rudquist, Liq. Cryst., 35, 789-791 (2008).